Chinese Journal of Polar Science, Vol. 8, No. 2, 79 - 88, December 1997

Atmospheric boundary layer structure and turbulent flux transfer over the Zhongshan Station area, Antarctica*

Qu Shaohou (曲绍厚), Gao Dengyi (高登义) and Zou Han (邹 捍)
Institute of Atmospheric Physics, Chinese Academy of Sciences, Beijing 100029, China

Received April 12, 1997

Abstract This article describes the atmospheric boundary layer structures and the turbulent flux transfers of heat and momentum over Zhongshan Station area, using Tethersonde Meteorological Tower (TMT) observation data, in the summer expedition of 1994 - 1995. With comparison of the atmospheric boundary layer structures and the turbulence transfers at three observation sites (with different topographic features) close to Zhongshan Station (69°22′S, 76°22′E), it is showed that the atmospheric boundary layer structure and the turbulence flux transfer are rather complicated and quite dependent on local topographic feature in Antarctica.

Key words atmospheric boundary layer, turbulent flux, air-ice(snow) interaction, flux-profile relation of similarity theory, Antarctica.

1 Introduction

The atmospheric boundary layer is a very important component in the atmosphere in which the heat, momentum and moisture exchanges are undergoing between the earth surface and the free atmosphere. The exchanges thereby have a significant impact on the publicly concerned climate change. However, the atmospheric boundary layer structure and the exchanges in it have quite local features that are determined by the underlying surface features. In the earth climate system, the exchanges of heat, momentum and moisture between the earth surface and the atmosphere can be on different interfaces, such as air-sea, air-snow, air-ice and air-land interfaces etc.. Antarctica, the snow-covered continent, has significant importance in controlling the atmospheric circulation by exchanges of heat, momentum and mass. The exchanges in Antarctica greatly influence the global climate. For instance, Xie *et al.* (1994) studied the relationship between the ENSO events and the sea ice in Antarctica, and got good results. As known, the surface of Antarctica is covered by snow and ice, and the exchanges are conducted mainly between the snow cover and the atmosphere. However, the exchanges of heat, momentum and mass can occur on the air-sea, air-land, air-snow and air-ice interfaces seasonally and partly in Antarctica. Attention should be paid on this different exchanges (from air-snow

* This work is supported by the National Natural Science Foundation of China (No. 49675252).

exchanges) to understand fully the heat, momentum and mass transferred between the Antarctica Continent and the atmosphere and to understand properly the effect of Antarctica on climate change. We have known more about the exchanges of the air-sea interface in oceanic regions (Qu 1993, 1996), but only a few works have been done on the Antarctica region (Zhou *et al.* 1990, Inoue 1989). This article attempts to describe the differences among the air-land, air-snow and air-sea ice exchanges in Antarctica, using the TMT observation system. It is helpful to understand the different structures of Antarctic atmospheric boundary layer and the exchanges of heat, momentum and mass in it.

2 The observation and calculation

2.1 The observation sites

Observation site A, Zhongshan Station (69° 22′S, 76°22′E, 17.7 m a.s.l.) is located in the Larsemann Hills. It was scattered with naked stones and sand as the underlying surface in summer, but is covered by snow and ice in other seasons. Hills are the main topography at this station. Therefore, the local wind system is very complicated, including mountain-valley wind, land-sea breeze and katabatic wind. The annual mean wind speed at this station is over 7 m/s, and the relative humidity about 50%. Observation site B is an ice cap site (69°25′S, 76°16′E, 200 m a.s.l.) with a main wind system of katabatic wind. Observation site C (69°21′S, 76°26′E) is located on the sea ice on the north of the Larsemann Hills. The three observation sites are shown in Fig. 1.

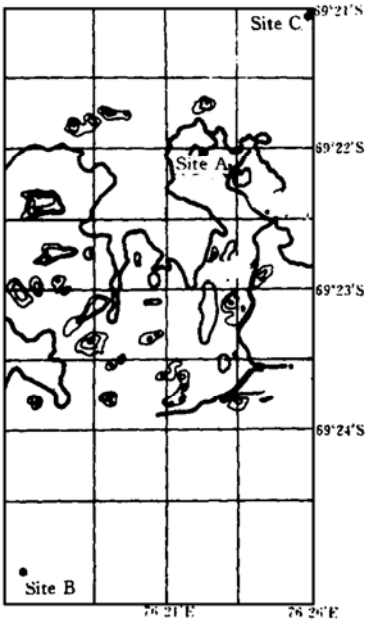

Fig. 1. The locations of the observation sites in the Zhongshan Station area.

2.2 Observation system

The Tethersonde Meteorological Tower (TMT) observation system used in this study includes air temperature, relative humidity, air pressure and wind observations at six levels. The maximum observation altitude is about 1500 m above the ground. The specifications of TMT is in Table 1.

Table 1. Specifications of TMT sounding system

Element	Range	Telemetric precision
Air temperature	−40 – 50℃	±0.3℃
Relative humidity	0 – 100%	±3%
Air pressure	600 – 1050 hPa	±0.5 hPa
Wind speed	0 – 20 m/s	±0.5 m/s
Wind direction	0 – 360°	±5°

2.3 Calculation

In the atmospheric boundary layer, the transfer of momentum and sensible heat in unit time and through unit area can be written as:

$$M=\rho\overline{w'u'}=-\rho u_*^2=-\rho K_M\frac{\partial\overline{u}}{\partial z}$$
$$H_s=c_p\rho\overline{w'\theta'}=-c_p\rho u_*\theta_*=-c_p\rho K_H\frac{\partial\overline{\theta}}{\partial z} \tag{1}$$

where ρ is the air density as a function of the air temperature and pressure, c_p the specified heat of dry air ($1.005\ \mathrm{Jg^{-1}\cdot K^{-1}}$), u_* the friction speed ($u_*^2=\overline{u'w'}=\tau\rho^{-1}$, τ the surface stress), θ_* the temperature scale ($\theta_*=-\overline{w'\theta'}\cdot u_*^{-1}$), u the wind speed, θ the potential temperature, $\overline{u}$the mean of wind speed, $\overline{\theta}$the mean of potential temperature, u′ the fluctuation of wind speed, θ' the fluctuation of potential temperature, K_M and K_H the eddy diffusivities for momentum and sensible heat, respectively.

According to the semi-empirical flux-profile relationship of Monin-Obukhov similarity theory, the wind shear and the temperature gradient can be described as functions of dimensionless height, $\varphi_M(\zeta)$ and $\varphi_H(\zeta)$, are written as the following:

$$\varphi_M(\zeta)=\frac{kz}{u_*}\frac{\partial\overline{u}}{\partial z}$$
$$\varphi_H(\zeta)=\frac{kz}{\theta_*}\frac{\partial\overline{\theta}}{\partial z} \tag{2}$$

where take $\zeta=z/L$ is the dimensionless height, $L=-Tu_*^3\cdot(\overline{gw'T'}k)^{-1}$ the Monin-Obukhov length, ($\zeta>0$ describes the stable atmosphere, and $\zeta<0$ the unstable), k von Kamen constant (here take $k=0.35$).

Using observation data of Air Force Cambridge, the empirical expressions of $\varphi_M(\zeta)$ and $\varphi_H(\zeta)$ can be written in the following forms:

$$\varphi_M(\zeta)=\begin{cases}1+\beta_m\zeta & (\zeta\geqslant 0)\\ (1-\gamma_m\zeta)^{-1/4} & (\zeta\leqslant 0)\end{cases} \tag{3}$$

$$\varphi_H(\zeta)=\begin{cases}1+\beta_n\zeta & (\zeta\geqslant 0)\\ (1-\gamma_n\zeta)^{-1/2} & (\zeta\leqslant 0)\end{cases} \tag{4}$$

where, $\beta_m=4.7$, $\gamma_m=15$, $\beta_n=6.4$ and $\gamma_n=9$.

Integrating equations (3) leads to the expression of wind profile:

when $\zeta<0$,

$$\frac{\overline{u}}{u_*}=\frac{1}{k}\left(\ln\frac{z}{z_0}-\Psi_1\right) \tag{5}$$

where, $\Psi_1=2\ln\left(\frac{1+x}{2}\right)+\ln\left(\frac{1+x^2}{2}\right)-2\mathrm{tg}^{-1}x+\frac{\pi}{2}$ and $x=(1-15\zeta)^{1/4}=\varphi_M^{-1}(\zeta)$;

when $\zeta>0$,

$$\frac{\overline{u}}{u_*}=\frac{1}{k}\left(\ln\frac{z}{z_0}+4.7\zeta\right) \tag{6}$$

Applying the same procedure to equation (4), the vertical temperature profile can be obtained as follows:

When $\zeta<0$,

$$\frac{\bar{\theta}-\theta_0}{\theta_*}=0.74\left(\ln\frac{z}{z_0}-\Psi_2\right) \tag{7}$$

where, $\Psi_2=2\ln\left(\frac{1+y}{2}\right)$, and $y=(1-9\zeta)^{1/2}=\varphi_H^{-1}(\zeta)$;

when $\zeta>0$,

$$\frac{\bar{\theta}-\theta_0}{\theta_*}=0.74\ln\frac{z}{z_0}+4.7\zeta \tag{8}$$

Based on these, profile data of mean wind and temperature are obtained by the TMT. Fitting the profiles to the equations (5) - (8) using least-square method, u_*, θ_* and z_0 are obtained, and the sensible heat and the momentum fluxes, H_s and M are calculated from equations (1).

3 Results and discussion

From the natures of the underlying surface, such as topography, landforms, geographical position and conditions of water and heat etc., the structure of the Antarctic atmospheric boundary layer can divided into three types:

(1) Ice cap atmospheric boundary layer with ice cap as the underlying surface;

(2) Land atmospheric boundary layer with naked stones and soil(mixed with ice or snow), especially in summer, as the underlying surface;

(3) Ocean atmospheric boundary layer with sea water, sea ice or their mixture as the underlying surface.

Studying the structure of the atmospheric boundary layer of Antarctica is to understand the heat, momentum and mass transfer between the underlying surface and the atmosphere in this region, and furthermore to understand the impact of the transfer on the climate change. The selected three observation sites during this Chinese summer survey can be the proxies of the three types of atmospheric boundary layers in Antarctica. Fig. 2, Fig. 3 and Fig. 4 demonstrate the wind and temperature evolution at the three observation sites.

In Fig. 2a, at 7 : 00 (curve 1) and 21 : 00 (curve 7), there was an inversion layer structure at the lower atmosphere at Zhongshan Station. The inversion intensity was about 0.45℃/10 m. At day time (curves 2, 3 and 4), the inversion layer was destroyed by the surface heating, and a mixing layer was formed at 40 m, raised to 120 m and vanished there. The lapse rate of temperature was about 0.9℃/100 m. This evolution of temperature profile is typically characterized as the land atmospheric boundary layer which can be observed in other continents as well (near surface inversion layer at night and mixing layer at daytime). Because of the complicated topography and air flows (might be the comprehensive impact from the mountain-valley wind, katabatic wind and land-sea breeze), the wind within 100 m from the underlying surface experienced a northeast-southwest-northwest-northeast shift. The wind in 100 m above the underlying surface reached 5 m/s at 7 : 00, and then the wind in 100 - 300 m speeded about 5 m/s. This could be the impact of the katabatic wind. However, the dominant wind was easterly (Fig. 2b).

From Fig. 3a and 3b (observation site B), it is shown that the inversion layer in near the ground surface appeared with the maximum height at 15 m and temperature difference about 0.5℃ (curve 1) at 14 : 00, the maximum height of the inversion layer raised up to 20 m with temperature difference about 1.0℃ at 16 : 00 (curve 2), the maximum height of the inversion layer continued to rise up to 40 m with the temperature difference about 2.0℃ at 17 : 00 (curve 3), the height of the inversion layer reached 100 m with the temperature difference about 2.0℃ at 23 : 00 (curve 6), and the maximum height of the inversion layer arrived at 130 m with the temperature difference about 2.0℃ at 01 : 00 next morning (curve 7). This phenomenon that the inversion layer (its intensity was about 0.35℃/10 m) exists in whole day, the temperature difference is enlarged in afternoon and the thickening of the inversion layer is highly related to the Antarctica katabatic wind. But the air temperature above this inversion layer was decreased with the height and its lapse rate of temperature was about 0.8℃/100 m. From the observation (Fig. 3b), the wind shear reached maximum at about 14 : 00, and the katabatic wind is dominant in the near surface layer with low speed. Afterwards, the wind shear became small, and the katabatic wind layer became greatest in thickness at 01 : 00 with the wind speed reaching the maximum (5 – 10 m/s) as compared with the minimum (1 – 2 m/s) at 14 : 00. Therefore, the cold katabatic wind is considered as the main cause of the whole-day inversion layer in the near surface layer, the katabatic wind makes the temperature near the surface layer decreasing, and thus causes the inversion layer thickened and strengthened. The katabatic wind, via the impact on the inversion layer, forms a downward

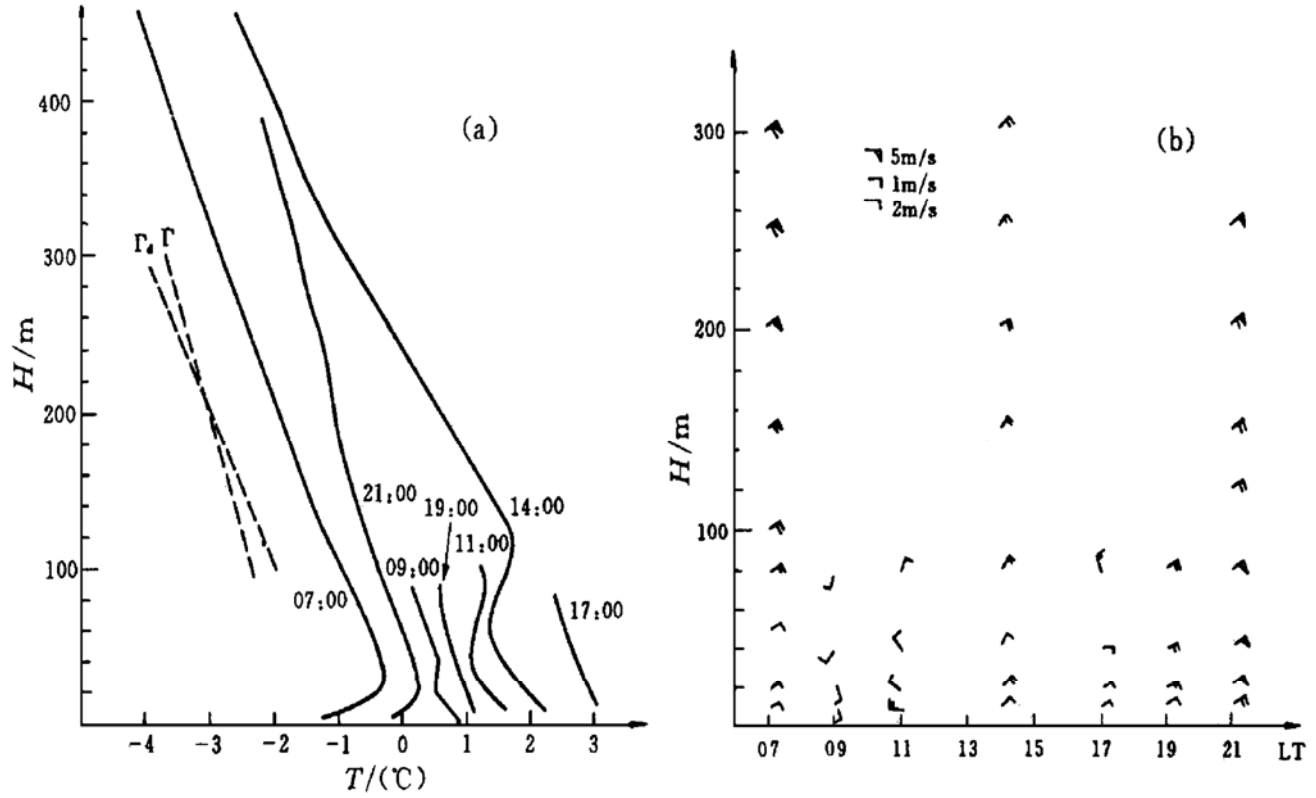

Fig. 2. Temporal-spatial variation for temperature profile (a) and wind profile (b) over Zhongshan Station.

transfer of heat flux over the Antarctica, and makes the continent as the largest cold source in the globe (discussed afterwards).

From the evolution of the vertical temperature distribution at the observation site C with sea-ice as the underlying surface (Fig. 4a), the inversion layer covered the area during 7 : 00 – 21 : 00 (inversion intensity was about 0.2℃/10 m), and the ceilling of the inversion layer gradully raised to 80 m or so. During the observation, the temperature of the mixed sea-ice, water and snow was stable with sea-ice thickness around 1 m. Therefore the vertical temperature difference was produced by the upper layer temperature that is decided by the air flows, oceanic one with higher temperature and continental one with lower temperature. From the Fig. 4b, it is shown that the northerly oceanic air flow during 07 : 00 – 10 : 00 caused the biggest inversion (curve 2), and the continental flow caused the inversion weakening after 12 : 00.

From the above discussion, it can be seen that the temperature profiles of the atmospheric boundary layer at the three observation sites have obvious differences in the near surface layer except that the temperature lapses (between the dry adiabatic lapse and the mean air temperature lapse) are similar in the upper layer. Observation site A, Zhongshan station, is located on the Ingrid Christensen coast of the peninsular and backed by ice sheet, and has more human activities. Therefore, the underlying surface is composed of naked stones and soil. The nature of naked soil-stone surface causes the highest daily range of temperature (12℃) among the three observation sites. The vertical temeperature structure and the diurnal variation controlled by

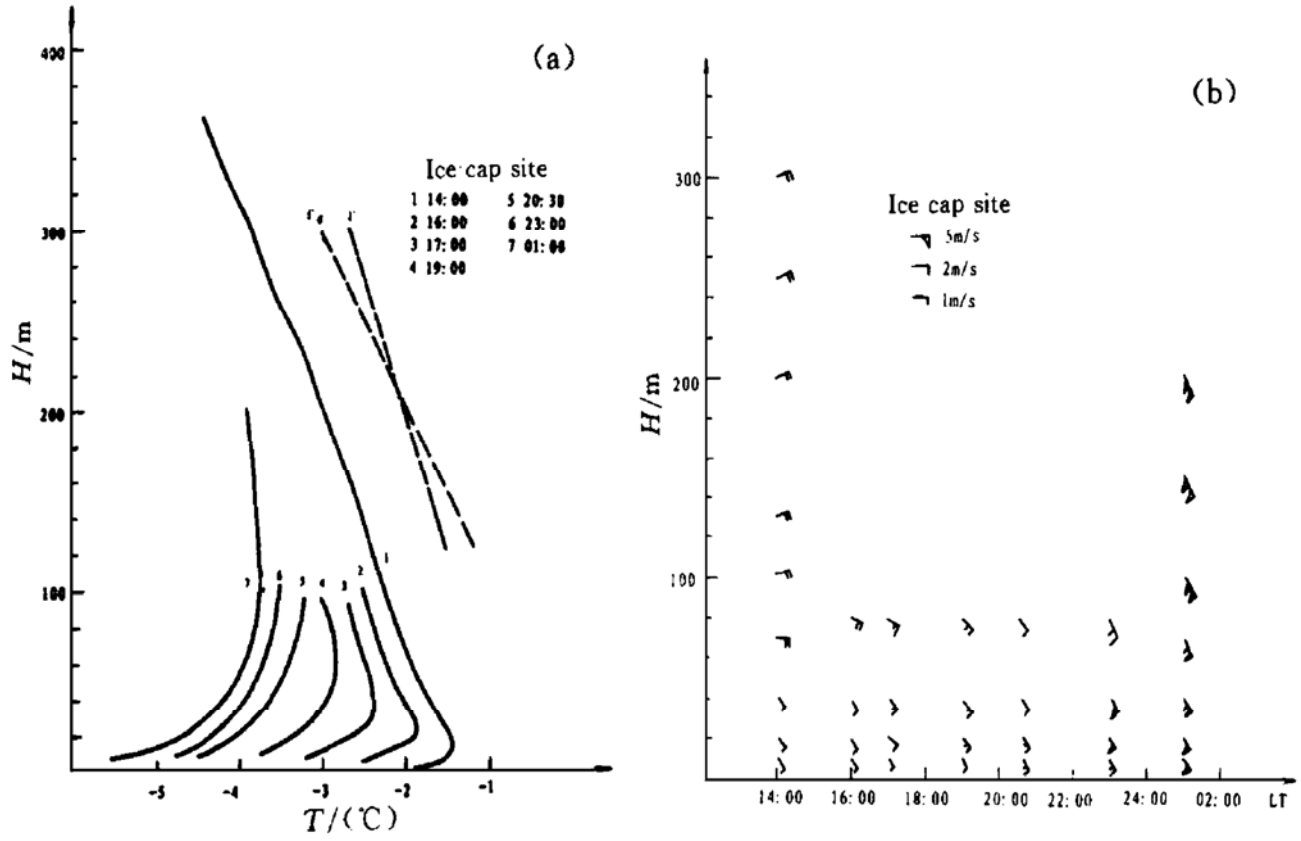

Fig. 3. Temporal-spatial variations for temperature profile (a) and wind profile (b) over the ice-cap site.

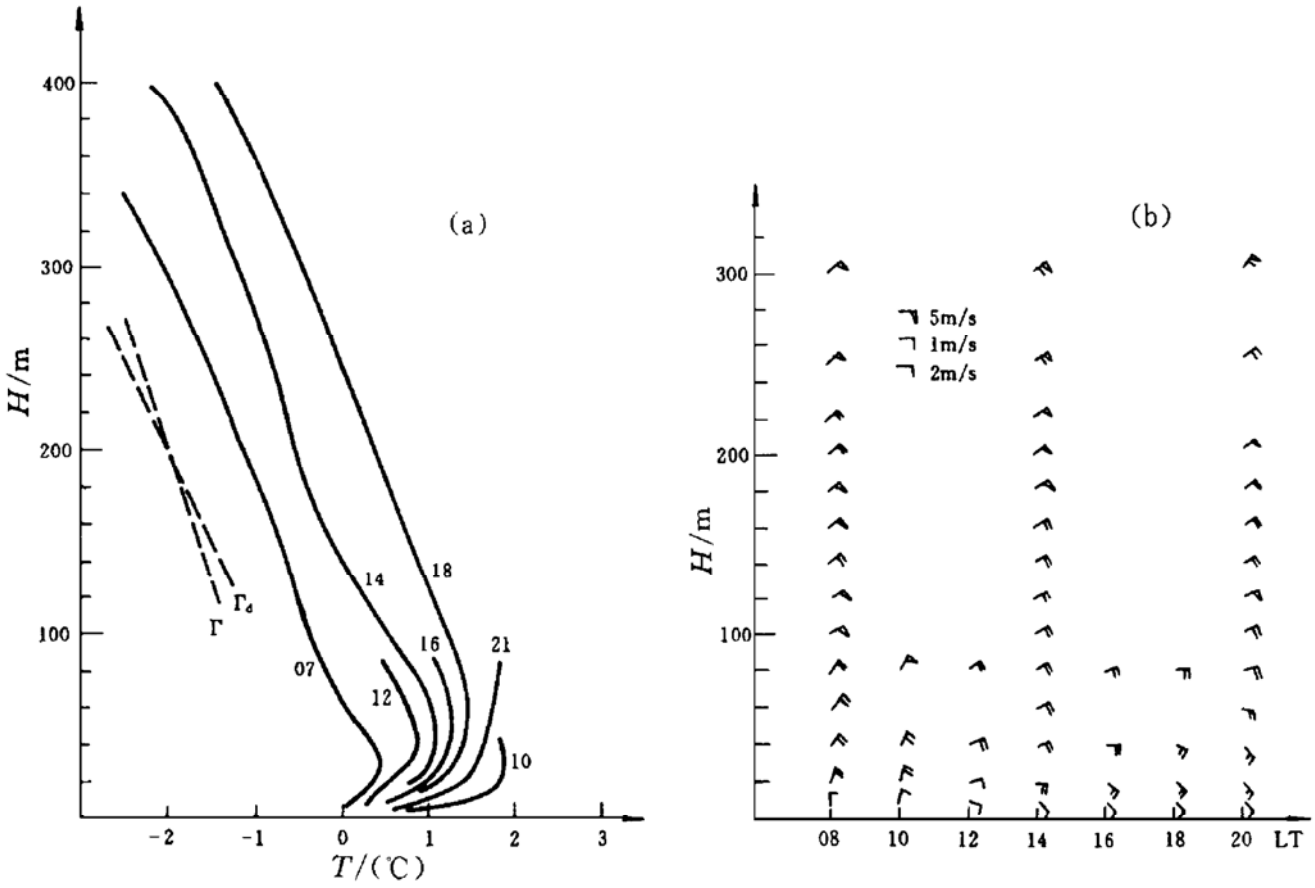

Fig. 4. Temporal-spatial variations for temperature profile (a) and wind profile (b) over sea-ice site.

the underlaying surface appear to be the typical continental land atmospheric boundary layer. At the observation site B, the ice cap point, the temperature inversion dominates at day time, and the daily range of temperature is about 8℃, being lower than that at the observation site A. The variation of the inversion layer is controlled by the katabatic wind that has direct impact on the vertical temperature distribution. At the observation site C, the inversion exists at most time of a day with weaker strength than those at the other observation sites. This is determined by the nature of the underlying surface. In summer, the thickness of sea-ice in this area is about 1 m with a relative high temperature, about 0℃ on the surface and decreasing, downwards to the sea water, to about −1℃. Meanwhile, the high heat capacity of the sea-ice and sea water keeps the diurnal variation of temperature within a small amplitude. The comparsion of the temperature profiles over Zhongshan Station area is shown in Table 2.

Table 2. Comparsion of the temperature profiles over the Zhongshan Station area

Sites	Lapes rate* Γ /−℃ · (100m)$^{-1}$	Inversion intensity γ /℃ · (10m)$^{-1}$	Daily range of temperature ΔT/℃	Thickness of inversion layer H/m
Sea ice	0.75	0.20	1 - 2	80
Ice cape	0.80	0.35	8	100
Zhongshan Station	0.90	0.45	12	120 (mixed layer)

* : dry adiabatic lapse rate $\Gamma_d = -0.965$℃/100 m; mean lapse rate of troposphere $\Gamma = -0.65$℃/100 m; wet adiabatic lapse rate $\Gamma_w = -0.40$℃/100 m (1000 hPa, 18℃).

Table 3. Turbulant transfer parameters at the observation sites

Site	Date		Time	z_0 /mm	R_i	ξ	$\overline{U}$ /m·s^{-1}	u_* /cm·s^{-1}	10^3M /N·m^{-2}	10^3C_D	θ_* /℃	H_s /W·m^{-2}
	month	day										
A	Dec.	21	7：00	15	0.07	0.15	1.6	10.0	9.8	3.90	0.06	−6.6
			9：00	32	−0.07	−0.08	2.0	14.5	20.7	5.26	−0.06	8.2
			11：00	35	−0.075	−0.09	2.4	17.7	30.9	5.44	−0.09	15.3
			14：00	37	−0.08	−0.10	3.5	26.1	67.1	5.56	−0.12	30.3
			17：00	30	−0.06	−0.07	1.5	10.7	11.0	5.09	−0.08	8.9
			19：00	**29**	−0.04	−0.05	2.5	17.8	31.2	**5.06**	−0.03	4.9
			21：00	13	0.06	0.10	4.0	24.4	58.7	3.72	0.07	−16.5
B	Dec.	17	14：00	**0.28**	0.11	0.28	1.8	6.6	4.3	**1.34**	0.09	−6.1
			16：00	0.30	0.12	0.30	2.2	8.1	6.4	1.36	0.11	−8.7
			17：00	0.27	0.13	0.39	2.5	9.1	8.2	1.32	0.13	−11.5
			19：00	0.075	0.14	0.50	2.8	9.0	8.0	1.03	0.09	−8.3
			20：30	0.025	0.16	0.75	2.5	7.3	5.3	0.85	0.11	−8.0
			23：00	0.19	0.13	0.39	5.0	17.6	30.5	1.24	0.17	−29.0
	Dec.	18	01：00	**0.28**	0.11	0.28	7.0	25.5	64.1	**1.33**	0.13	−32.9
C	Jan.	12	07：00	0.034	0.11	0.28	2.5	7.5	5.5	0.91	0.02	−1.5
			10：00	0.005	0.18	0.80	3.0	7.7	5.8	0.66	0.13	−9.9
			12：00	**0.36**	0.06	0.10	3.2	12.0	14.2	**1.41**	0.04	−4.7
			14：00	0.20	0.07	0.15	2.8	9.9	9.7	1.25	0.07	−6.8
			16：00	0.094	0.10	0.26	2.1	6.9	4.7	1.08	0.09	−5.4
			18：00	0.081	0.12	0.30	2.5	8.1	6.4	1.05	0.14	−11.2
			21：00	0.079	0.10	0.26	3.0	9.7	9.3	1.05	0.10	−9.6

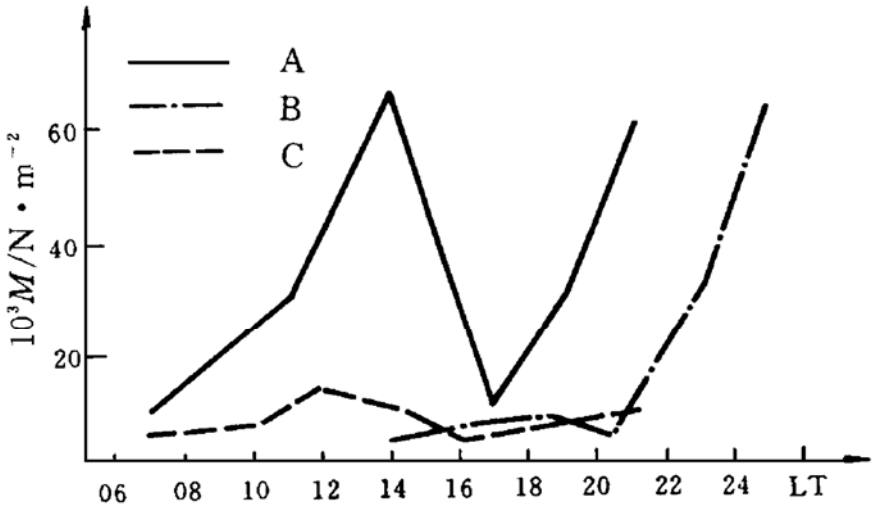

Fig. 5. Transfer characteristics of the momentum flux over the Zhongshan Station area.

The turbulence transfer characteristics, the roughness parameter z_0, the Richardson number R_i, the friction speed u_*, the momentum flux M, the drag coefficient C_D, the temperature scale θ_*, the sensible heat flux H_S, in the atmospheric boundary layers at the three observation sites are listed in Table 3. The roughness parameters at the three observation sites are quite different. The values at observation sites A, B and C are 29 mm, 0.28 mm and 0.36 mm, respectively for near the neutral conditions. The differences are caused by the topography and the composition of the underlying surfaces. The downward momentum transfer is different at the three sites. The maximum is at the observation site A (Fig. 5). Since the momen-

tum transfer is related (Equation (1)) to the friction speed, and the friction speed is linked with the roughness parameter, the momentum transfer is related to the nature of the underlying surface. At a same location, the momentum transfer is positively related to the wind speed. The larger the wind speed and the wind shear, the more momentum transferred downwards. For instance, the wind speed experienced the maximum, 5 – 7 m/s, during 23 : 00 Dec. 17 – 01 : 00 Dec. 18, and at meantime the momentum transfer reached the maximum. The drag coefficients C_D at the sites A, B and C are respectively 5.06×10^{-3}, 1.33×10^{-3} and 1.41×10^{-3}, for the near neutral conditions. This is because C_D is related to the z_0 that explains the nature of the underlying surface. The drag coefficient is related to the Richardson number as well. Under the neutral conditions, The smaller R_i, the larger C_D when R_i is less than zero (unstable atmosphere), and the larger R_i, the smaller C_D when R_i is greater than zero (stable atmosphere).

The sensible heat transfer at the three observation sites is illustrated in Fig. 6. The sensible heat flux transferred to the atmosphere is different at the three observation sites. The sensible heat flux at site A during 7 : 00 – 19 : 00 was positive, but it was negative at other time. In other words, the underlying surface was heat source during 7 : 00 – 19 : 00 and cool source at other time. The shift between heat and cool sources is related to the temperature stratification in the near surface layer (Fig. 2a). When the inversion layer was established, the flux was downward (the surface became a cooling source). When the temperature decreased with height (higher mixing layer), the flux was upward (the surface was a heating source). The magnitude of the heat flux is determined by the temperature difference described by temperature scale θ_* and the friction speed u_* (Table 2). The sensible heat fluxes at the observation sites B and C were downward, i. e., the heat was transferred from the atmosphere to the surface. The difference between the site B and the site C was that the katabatic wind made the heat flux increasing rapidly, from 8.0 W/m^2 to 30 W/m^2, at 23 : 00 and 01 : 00.

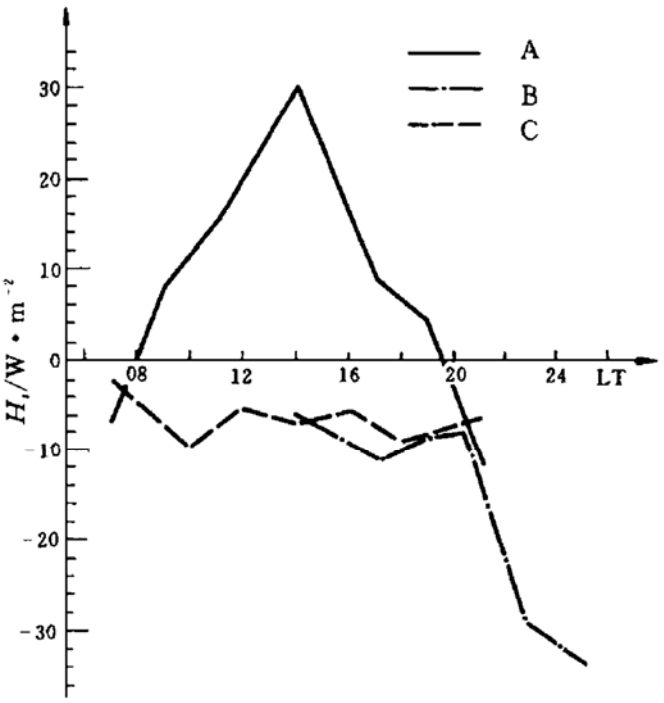

Fig. 6. Transfer characteristics of the sensible heat flux over the Zhongshan Station area.

4 Conclusions

In general, the Antarctica is a cooling source to the atmosphere, which has important impact on the climate and the weather system. However, the characteristics of atmospheric boundary layer vary with the location along the coast region, especial-

ly in summer.

(1) The region around Chinese Zhongshan Station has very complicated underlying surface with the Antarctic glacier, neo-snow-coverred sea-ice and naked stones and soil. The structure of the atmospheric boundary layer in this region varies with the heating nature of the surface, topography and landforms. However, the temperature structure is the main point to decide if the underlying surface is a heating or cooling source.

At the observation site B, or the ice cap site, in the near surface layer there was a inversion layer whose ceiling raised from 10 m to 130 m with strength increasing, during 14 : 00 - 01 : 00 (Fig. 3a). This process is related to the katabatic wind. On the neo-snow-covered sea-ice, the inversion experienced weak-strong-weak-strong change in the period of 07 : 00 - 09 : 00, 09 : 00 - 14 : 00 and 14 : 00 - 21 : 00. This porcess is related to the wind variation (e. g. sea breeze) over this region. At the site A, or on the naked stones and soil, the vertical temperature structure was the mixed and unstable layers, except the inversion layer from 21 : 00 to 07 : 00. This is similar to the atmospheric boundary layer over land.

Over the neo-snow-covered sea-ice, there was multi-layer inversion in the layer from the surface to 100 m (Fig. 4a). This is possibly related to the different heating due to the phase change of the new snow.

(2) In the Zhongshan Station region, the roughness length is the maximum at the observation site A and not quite defferent from those at site B and C. The value of drag coefficient is 5.06×10^{-3} with maximum over the naked stones and soil, and those are 1.33×10^{-3} and 1.41×10^{-3} over the sea ice and the ice cap. The drag coefficient is related to the mean wind speed and Richardson number besides the roughness length.

(3) The downward momentum transfer is mainly related to the average wind speed besides the roughness.

Acknowledgment The authors are indebted to Gao Xuejie, Wang Wendong, Zhang Jinding and Wang Xinmin for assistance in this study and field work.

References

Inoue J (1989): Surface drag over the snow surface of the Antarctic Plateau. J. Geophys. Res., 94(D2): 2207 - 2224.

Qu SH (1993): Different characteristics of turbulant fluxes transfer over the western tropic pacific ocean in El Nino and Non-El Nino years. Chinese J. Atmos. Sci., 17(3): 259 - 267.

Qu SH (1996): Turbulent flux transfer over the western tropical pacific ocean during westerly burst. Chinese J. Atmos. Sci., 20(2): 161 - 167.

Xie SM, Bao CL, Xue ZH, Zhang L, Hao CJ (1994): Interaction between Antarctic sea ice and ENSO events. Proccedings of the NIPR Symposium on Polar Meteorology and Glaciology, National Institute of Polar Research, Tokyo, No. 8 : 95 - 110.

Zhou XJ, Bian LG, Jia PQ, Lu LH (1990): A preliminary study on surface thermal regime of the Great Wall Station. Chinese Science Bulletin, 35 (19): 1638 - 1642.